

Solvothermal synthesis and characterization of silica-pillared titanium phosphate

Xiuling Jiao,^a Dairong Chen,^b Wenqin Pang,^{a*} Ruren Xu^a and Yong Yue^c

^aDepartment of Chemistry, Jilin University, Changchun 130023, PR China

^bDepartment of Chemistry, Shandong University, Jinan 250100, PR China

^cWuhan Institute of Physics, The Chinese Academy of Science, Wuhan 430071, PR China

Received 15th April 1998, Accepted 4th August 1998

Silica-pillared titanium phosphate has been synthesized from $\text{Ti}(\text{OC}_4\text{H}_9)_4\text{-H}_3\text{PO}_4\text{-H}_2\text{N}(\text{CH}_2)_3\text{Si}(\text{OC}_2\text{H}_5)_3\text{-C}_2\text{H}_5\text{OH}$ and characterized by XRD, SEM, IR and TGA. The synthesis conditions were investigated and the optimal conditions are reported: crystallization at 180 °C for about 7 days with a batch composition of 1.0 $\text{Ti}(\text{OC}_4\text{H}_9)_4$:3.6 H_3PO_4 :1.0 $\text{H}_2\text{N}(\text{CH}_2)_3\text{Si}(\text{OC}_2\text{H}_5)_3$:33 $\text{C}_2\text{H}_5\text{OH}$. XRD analysis gives the lattice parameters of the monoclinic cell as $a = 1.99952$ nm, $b = 0.41803$ nm, $c = 0.90062$ nm, $\beta = 97.462^\circ$, $V = 0.74642$ nm³, and $Z = 2$. N_2 adsorption-desorption test shows that the pillared compound has a BET surface area of 51 m² g⁻¹.

Introduction

Pillaring of layered compounds such as clay minerals, oxides and phosphates has been extensively studied for the last decade.¹⁻⁵ Since the first preparative studies by Clearfield *et al.*⁶ and Alberti *et al.*⁷ of α -ZrP, many works have focused on the syntheses and characterization of pillared layered metal(IV) phosphates,^{8,9} and a review discussed the preparation, characterization and properties of pillared layered metal(IV) phosphates.¹⁰ Generally, the pillared compounds are prepared by ion exchange of polynuclear species or by the hydrolysis of organometallic precursors, such as $[\text{Al}_{13}\text{O}_4(\text{OH})_{24}(\text{H}_2\text{O})_{12}]^{7+}$, $\text{R}_x\text{Si}(\text{OR}')_{4-x}$ *etc.*, using the sol-gel method; several pillared metal phosphates such as silica-pillared α -ZrP,¹¹ silica-pillared α -SnP,¹² Al-pillared α -ZrP¹³ *etc.*^{14,15} have been obtained. However, intercalation of large cations into the interlayer space often results in a low yield and low crystallinity of the pillared compounds. For example, well crystallized silica-pillared titanium phosphate can not be obtained by this method.^{11,12}

Here, we report a new route for the synthesis of well crystallized silica-pillared layered titanium phosphate. The pillared compound is hydrothermally synthesized in $\text{Ti}(\text{OC}_4\text{H}_9)_4\text{-H}_3\text{PO}_4\text{-H}_2\text{N}(\text{CH}_2)_3\text{Si}(\text{OC}_2\text{H}_5)_3\text{-C}_2\text{H}_5\text{OH}$, and the product obtained by this method has a high crystallinity.

Experimental

1. Synthesis

All the reagents were of analytical grade and were not further purified before utilization.

Tetrabutyltitanate (analytical reagent, TBOT), phosphoric acid (analytical reagent, 85 wt.%) and 3-aminopropyltriethoxysilane (APTEOS, Aldrich) were used as titanium, phosphorus and silica sources. To adjust the hydrolysis and polymerization rate of APTEOS in the hydrothermal process, ethanol (EA, analytical reagent, 99.7%) was selected as the solvent. In a typical synthesis, phosphoric acid was added to a homogeneously mixed solution of TBOT and EA under stirring. APTEOS was added dropwise to this mixture and a white gel formed. The gel was placed into a Teflon-lined stainless steel autoclave and heated to 140–240 °C for about 7 days. It was then cooled to room temperature and the product was recovered by filtration, thoroughly washed with deionized water, and dried at room temperature.

2. Characterization

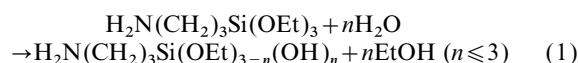
XRD patterns of the products were recorded with a Rigaku D/MAX-III diffractometer using Cu-K α radiation ($\lambda = 0.15418$ nm) at room temperature over the range 3–60°. Infrared spectra were measured on a Nicolet 5DX FT-IR instrument using the KBr pellet technique. ¹³C, ²⁹Si, ³¹P MAS NMR spectra were recorded on a Bruker MSL-400 spectrometer. Inductive coupled plasma analyses (ICP) for the Ti, P, Si contents in the product were obtained from a Leeman ICP-AES instrument, and elemental analyses for C, H, N contents were done on a Perkin-Elmer 240C elemental analyzer. Thermogravimetric analyses (TGA) were performed on a Perkin-Elmer TGA7 with increasing temperature rate of 10 °C min⁻¹. Water adsorption measurements were carried out on a Cahn 2000 vacuum electron balance at room temperature, while N_2 adsorption-desorption and BET surface area on the calcined sample (77 K) were measured on an ASAP 2010 micromeritics apparatus.

Results and discussion

1. Synthesis

The crystalline pillared compound was synthesized from the batch composition 1.0 TBOT:(2.0–5.0) H_3PO_4 :1.0 APTEOS:33 EA at 140–240 °C for several days.

Hydrolysis may occur in the mixed gel as follows:



The hydrolyzed APTEOS then polymerizes continuously. To adjust the rate of hydrolysis and polymerization, ethanol (99.7%) was used as the solvent. The title compound could not be obtained with ethanol (95%) or water as solvent. Further experiments indicated that the crystallization reaction accelerated upon increasing the H_3PO_4 content in gel mixture, and an unknown phase formed when the reaction time was prolonged to 15 days. Crystallization at 180 °C for about 7 days with the batch composition of 1.0TBOT:3.6 H_3PO_4 :1.0 APTEOS:33 EA was optimal.

2. Characterization

Fig. 1 shows the SEM of the as-prepared crystals. The crystals are homogeneous with sheet-like morphology indicating that the solid is phase pure. The average particle size is about 2 μm .

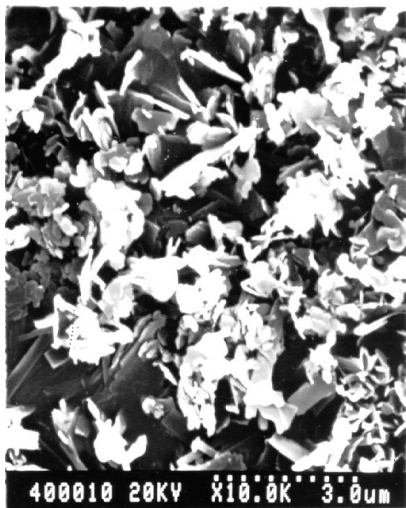


Fig. 1 Scanning electron micrograph of as-synthesized powder.

Fig. 2 gives the XRD pattern of the title compound. The product recovered is of high crystallinity. It can be seen from Fig. 2 that the XRD pattern of the as-prepared product is similar to that of the γ -phase structure,^{14,16} although the peak positions and intensities are different. Because of the replacement of H_3O^+ in the interlayer space of γ -TiP by $\text{NH}_3^+(\text{CH}_2)_3(\text{O})\text{SiOSi}(\text{O})(\text{CH}_2)_3\text{NH}_3^+$ in the title compound, the basal spacing of the as-prepared product is much larger than that of γ -TiP. This replacement further leads to a change of β value and an increase of the unit cell volume. The similarity of the layer structures of γ -TiP and the title compound can also be seen from the XRD patterns, although the basal space reflections are different. We therefore assume that the layer structure of the as-synthesized product is similar to that of γ -TiP. The difference between the XRD patterns can be attributed to the influence of the silica pillar to the phosphate layer, and even to the lattice structure of the crystal. The X-ray powder diffraction data were indexed with the TREOR program (Table 1). The cell is monoclinic with $a=1.99952$ nm, $b=0.41803$ nm, $c=0.90062$ nm, $\beta=97.462^\circ$ and

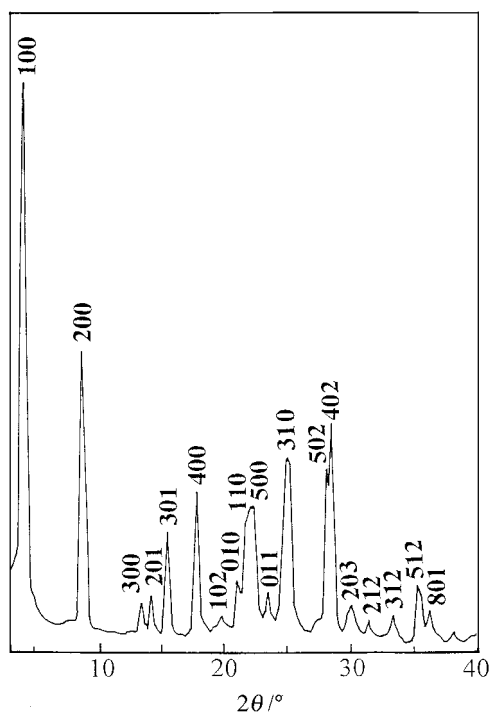


Fig. 2 XRD pattern of the title compound.

Table 1 X-Ray powder diffraction data and indexing results of silica-pillared layered titanium phosphate

<i>h</i>	<i>k</i>	<i>l</i>	$d_{\text{obs}}/\text{\AA}$	$d_{\text{calc}}/\text{\AA}$	$2\theta_{\text{obs}}/^\circ$	$2\theta_{\text{calc}}/^\circ$
1	0	0	19.87	19.83	4.443	4.453
2	0	0	9.94	9.91	8.889	8.913
3	0	0	6.60	6.61	13.405	13.387
2	0	1	6.25	6.24	14.159	14.173
3	0	1	5.71	5.67	15.506	15.599
4	0	0	4.95	4.96	17.905	17.881
1	0	2	4.50	4.48	19.713	19.791
0	1	0	4.20	4.18	21.136	21.237
1	1	0	4.07	4.09	21.820	21.709
5	0	0	3.97	3.97	22.376	22.404
0	1	1	3.79	3.79	23.454	23.479
3	1	0	3.53	3.53	25.208	25.188
5	0	2	3.17	3.18	28.127	28.066
4	0	2	3.12	3.12	28.587	28.569
2	0	3	2.96	2.96	30.168	30.182
2	1	2	2.85	2.85	31.362	31.403
3	1	2	2.68	2.68	33.408	33.390
5	1	2	2.53	2.53	35.352	35.463
8	0	1	2.47	2.47	36.343	36.310

$V=0.74642$ nm³. From the unit cell parameters and the P—O and Ti—O bond lengths and the structure of layered titanium phosphate, the result of $Z=2$ can be obtained.

Further experiments shows that no significant change of the interlayer spacing is observed when the calcination temperature is lower than 300 °C, and the significant change of the basal spacing takes place between 300 and 500 °C, decreasing from 1.93 nm to 1.42 nm. Upon increasing the calcination temperature, the basal spacing decreases to 1.40 nm. The pillared compound is stable up to 700 °C (Fig. 3).

The ¹³C MAS NMR spectrum (Fig. 4) exhibits three peaks at 42.96, 20.99, and 10.21 ppm, which are attributed to C_α, C_β and C_γ in $\text{H}_3\text{N}^+\text{C}_\alpha\text{H}_2\text{C}_\beta\text{H}_2\text{C}_\gamma\text{H}_2\text{Si}$, respectively,¹⁷ which indicates that EA and other organic materials do not exist in the product. The disappearance of these resonances after calcination at 600 °C reveals that the organic material is lost at 600 °C.

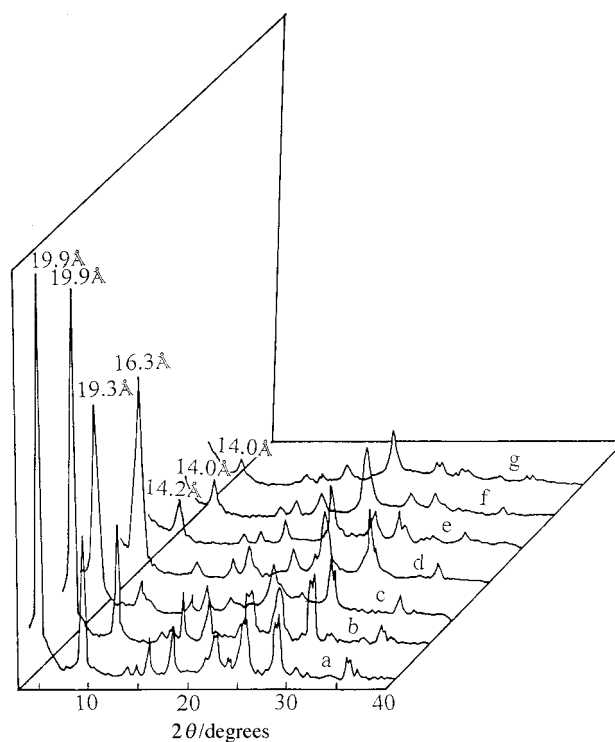


Fig. 3 XRD patterns of as-prepared samples (a), and of samples calcined at 200 (b), 300 (c), 400 (d), 500 (e), 600 (f), 700 °C (g).

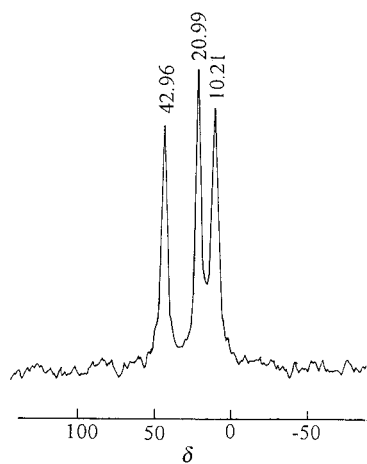


Fig. 4 ^{13}C MAS NMR spectrum of as-prepared product (from TMS).

^{29}Si CP MAS NMR spectra (Fig. 5) for as-synthesized and calcined products have two resonances at -66.80 and -103.85 ppm, which are assigned to the silicon atoms as shown in Fig. 6.¹⁸ This result confirms that APTEOS is thoroughly hydrolyzed and polymerized.

^{31}P MAS NMR spectra (Fig. 7) of the powder give two resonances at -12.95 , -25.22 ppm with an intensity ratio of

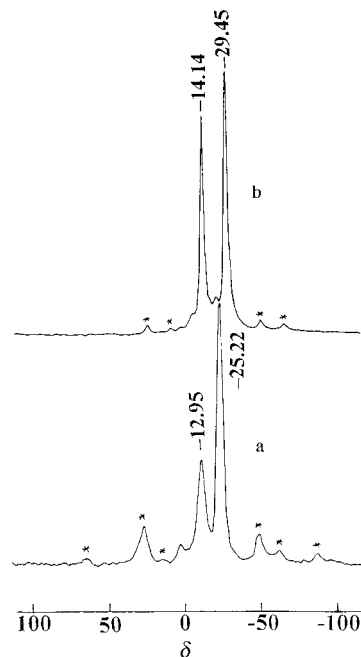


Fig. 7 ^{31}P MAS NMR spectra of as-prepared (a) and calcined (b) samples (from H_3PO_4).

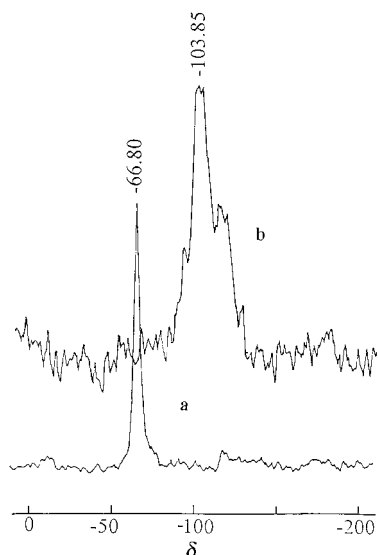


Fig. 5 ^{29}Si CP MAS NMR spectra for as-prepared (a) and calcined (b) product (from TMS).

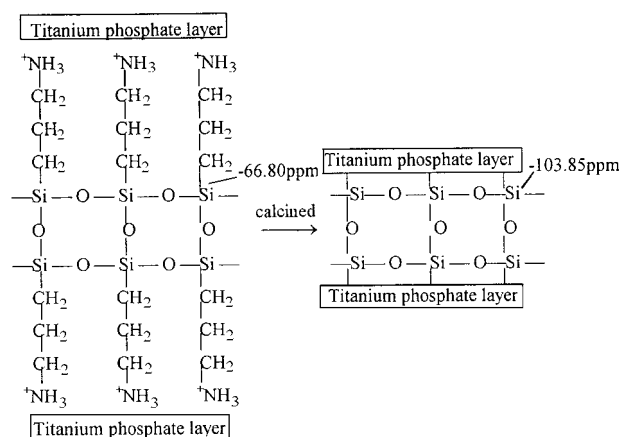


Fig. 6 Schematic representation of the product.

about 1:2, which shift to -14.14 and -29.45 ppm after calcination at 500°C for 3 h with a peak area ratio of 1:1. The ^{31}P MAS NMR spectrum of intercalated α -phase structure metal(IV) phosphates either have a single resonance or have several similar shifts,^{1,10,12,13,19} although there are two crystallographically inequivalent P sites in the structure, and only after thermal treatment are two ^{31}P shifts obtained.¹ Thus from the two ^{31}P resonances of the as-prepared compound and the shape of the shifts, these peaks should be assigned to two different phosphorus atoms— $\text{P}(\text{OTi})_2(\text{OH})_2$ and $\text{P}(\text{OTi})_4$.²⁰ This indicates that the structure of the phosphate layer is similar to that of γ -TiP, which also has these two different phosphorus atoms. After calcination, the two resonances shift to -14.14 and -29.45 ppm and the area ratio changes to about 1:1, these resonances can be attributed to $\text{P}(\text{OTi})_2(\text{OH})(\text{OSi})$ and $\text{P}(\text{OTi})_4$. The replacement of OH with OSi causes the resonances to shift from -12.95 and -25.22 ppm to -14.14 and -29.45 ppm, and the area ratio of these resonances for the calcined sample is consistent with the P/Si ratio in the product, *i.e.* only half of the P are linked to OSi—the molar ratio of $\text{P}(\text{OTi})_2(\text{OH})(\text{OSi})$ to $\text{P}(\text{OTi})_4$ is 1:1.

Fig. 8 shows the IR spectra of as-synthesized samples and those heated to 200, 300, 400, 500, 600, 700 $^\circ\text{C}$, respectively. The bands for the as-synthesized sample are assigned as follows: 3479, hydrogen bound OH; 3261, NH_3^+ stretching; 2917, CH_2 stretching; 1623, NH_3^+ asymmetric deformation H_2O bending; 1525, NH_3^+ ; 1475, CH_2 bending; 1398, P—O; 1215, C—C—N; 1152, P—O; 1004, P—O; 962, Si—O—Si; 798, NH_3^+ in-plane rocking; 701, NH_3^+ out-of-plane deformation; 646, Ti—O; 549, 512, 470, Ti—O. No significant changes of the spectra were observed below 300 $^\circ\text{C}$ except for the shift of the bands around 1000–900 cm^{-1} , indicating the distortion of the structure. Significant changes of the spectra above 300 $^\circ\text{C}$ result from the decomposition and loss of organic materials.

The weight loss from room temperature to 300 $^\circ\text{C}$ (about 3%, Fig. 9) is assigned to the loss of water in the interlayer space, while that from 300–600 $^\circ\text{C}$ (about 19%) is attributed to the loss of the organic material. The weight loss between

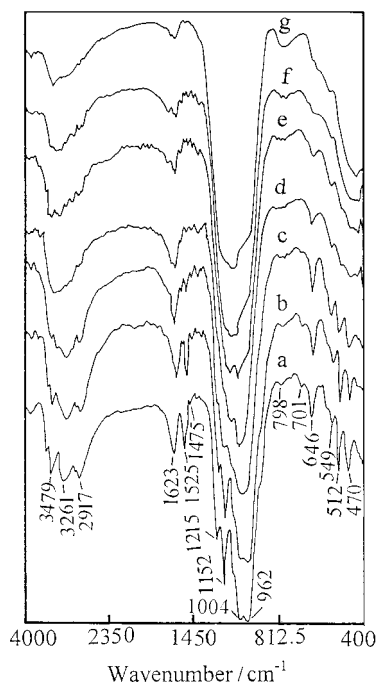


Fig. 8 IR spectra of as-prepared samples (a), and of samples calcined at 200 (b), 300 (c), 400 (d), 500 (e), 600 (f), 700 °C (g).

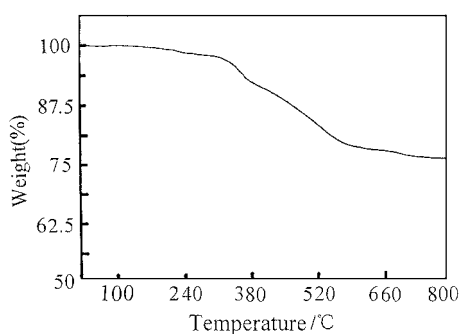


Fig. 9 TGA curve of the title compound.

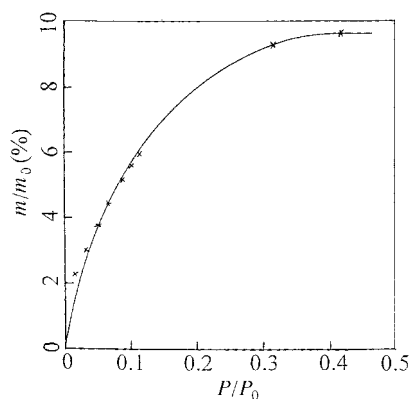


Fig. 10 Water adsorption isotherm of the sample calcined at 600 °C.

644 and 732 °C is attributed to the loss of water from the silanol groups.

N₂ adsorption–desorption tests indicate a BET surface area of ca. 51 m² g⁻¹ and the amount of N₂ adsorption is small. From the basal spacing of the calcined sample, the interlayer space is about 7 Å, which is large enough to adsorb the N₂ molecules. The interlayer region is occupied by the silica pillar for each P(OTi)₂(OH)₂ is connected to one silica pillar, which prevents the N₂ molecules from entering. The results further indicate that there are no mesopores in the calcined product, as there is little hysteresis on the N₂ adsorption–desorption curve when P/P₀ is higher than 0.5, which shows that the pillared phosphate is a cross-linked compound rather than a porous one. However, adsorption of water shows that the pillared compound (600 °C, 0.5 h) has the capacity to adsorb small polar molecules. The uptake of water at P/P₀=0.3 is as high as about 10% by weight. Fig. 10 shows the water adsorption isotherm of the sample.

We thank the National Natural Scientific Foundation and the Key Laboratory of Synthesis and Preparative Chemistry, Jilin University for financial support.

References

- 1 L. Li, X. Liu, Y. Ge, L. Li and J. Klinowski, *J. Phys. Chem.*, 1991, **95**, 5910.
- 2 W. L. Ijdo, T. Lee and T. J. Pinnavaia, *Adv. Mater.*, 1996, **8**, 79.
- 3 A. Kudo and T. Sakata, *J. Mater. Chem.*, 1993, **3**, 1081.
- 4 F. J. Perez-Reina, P. Olivera-Pastor, E. Rodríguez-Castellón and A. Jiménez-López, *J. Solid State Chem.*, 1996, **122**, 231.
- 5 A. Espina, J. B. Parra, J. R. García, J. A. Pajares and J. Rodríguez, *Mater. Chem. Phys.*, 1993, **35**, 250.
- 6 A. Clearfield and B. D. Roberts, *Inorg. Chem.*, 1988, **27**, 3237.
- 7 G. Alberti, U. Costantino, R. Vivani and P. Zappelli, *Mater. Res. Soc. Symp. Proc.*, 1991, **233**, 95.
- 8 A. Guerrero-Ruiz, I. Rodríguez-Ramos, J. L. G. Fierro, A. Jiménez-López, P. Olivera-Pastor and P. Maireles-Torres, *Appl. Catal. A*, 1992, **92**, 81.
- 9 G. Alberti, F. Marmottini, S. Murcia-Mascarós and R. Vivani, *Angew. Chem., Int. Ed. Engl.*, 1994, **33**, 1594.
- 10 P. Olivera-Pastor, P. Maireles-Torres, E. Rodríguez-Castellón, A. Jiménez-López, T. Cassagneau, D. J. Jones, and J. Rozière, *Chem. Mater.*, 1996, **8**, 1758.
- 11 J. Rozière, D. J. Jones and T. Cassagneau, *J. Mater. Chem.*, 1991, **1**, 1081.
- 12 P. Sylvester, R. Cahill and A. Clearfield, *Chem. Mater.*, 1994, **6**, 1890.
- 13 J. M. Mérida-Robles, P. Olivera-Pastor, A. Jiménez-López and E. Rodríguez-Castellón, *J. Phys. Chem.*, 1996, **100**, 14726.
- 14 T. Cassagneau, D. J. Jones and J. Rozière, *J. Phys. Chem.*, 1993, **97**, 8678.
- 15 M. Alcántara-Rodríguez, P. Olivera-Pastor, E. Rodríguez-Castellón, and A. Jiménez-López, *J. Mater. Chem.*, 1996, **6**, 247.
- 16 A. N. Christensen, E. K. Andersen, I. G. K. Andersen, G. Alberti, M. Nielsen and M. S. Lehmann, *Acta Chem. Scand.*, 1990, **44**, 865.
- 17 E. Bayer, K. Albert, J. Reiners, M. Nieder and D. Müller, *J. Chromatogr.*, 1983, **264**, 197.
- 18 G. E. Maciel, P. W. Sindorf and V. J. Bartuska, *J. Chromatogr.*, 1981, **205**, 438.
- 19 D. J. MacLachlan and K. R. Morgan, *J. Phys. Chem.*, 1990, **94**, 7656.
- 20 N. J. Clayden, *J. Chem. Soc., Dalton Trans.*, 1987, 1877.